C.P. No. 159
(15,625)
A R C Technical Report



MINISTRY OF SUPPLY

AERONAUTICAL RESEARCH COUNCIL

CURRENT PAPERS

# An Investigation into the Rolling Power and Aileron Reversal Characteristics of Swept Wings

By

A. V. Colès, B.Sc, and R. J Margetts, B.Sc

LONDON . HER MAJESTY'S STATIONERY OFFICE

1954

Price 2s 6d net

C.P. No. 159

UNIVERSITY OF BRISTOL
Department of Aeronautical Engineering
REPORT No. 11

# AN INVESTIGATION INTO THE ROLLING POWER AND AILERON REVERSAL CHARACTERISTICS OF SWEPT WINGS

- By -

A. V. Coles, B.Sc.
and
R. J. Margetts, B.Sc.

SUMMARY

The introduction of sweptback wings has made it necessary to extend the aeroelastic theories developed for aileron reversal of straight wings. The present paper reviews briefly existing theories relating to swept wings and presents the results obtained from a programme of tests on flexible swept wings.

The wings tested were of constant span, aspect ratio and area and had angles of sweep ranging from 15° sweepforward to 60° sweepback. The tests were carried out in a low-speed wind-tunnel, compressibility effects being absent.

The test results showed that the reversal speeds of wings of the same stiffness increase with both sweepback and sweepforward, the minimum value occurring with a small amount of sweepback. Predictions of reversal speeds based on semi-rigid theory showed good agreement with experimental results.

CONTENTS

## LIST OF SYMBOLS

| | |
|---|---|
| $a_1$ | $\frac{\partial C_L}{\partial \alpha}$ (Variation of Lift Coefficient with Incidence) |
| $a_2$ | $\frac{\partial C_L}{\partial \xi}$ (Variation of Lift Coefficient with Aileron Angle) |
| $c$ | Wing Chord |
| $\bar{c}$ | Mean Wing Chord |
| $C_l$ | Rolling Moment Coefficient |
| $C_L$ | Lift Coefficient |
| $C_m$ | Pitching Moment Coefficient |
| $e$ | Distance of flexural centre behind aerodynamic centre as a fraction of wing chord |
| $f(\eta)$ | Twist function defining variation of twist along span |
| $l_\phi$ | Bending Stiffness of Wing in lb ft per radian |
| $m$ | $-\left[\frac{\partial C_m}{\partial \xi}\right]_{C_L \text{ const.}}$ (Variation of Pitching Moment Coefficient with aileron angle at constant Lift Coefficient) |
| $m_\theta$ | Torsional Stiffness of Wing in lb ft per radian |
| $p$ | Rolling Velocity in radians per second |
| $q$ | Dynamic Head in lb per sq ft |
| $q_r$ | Dynamic Head at reversal |
| $s$ | Semi Span of Wing |
| $T$ | Constant defining position of flexural axis |
| $V$ | Airspeed in ft per second |
| $x$, $y$, $z$ | Co-ordinate Axes |
| $\gamma$ | Angle of Sweep, positive for sweepback |
| $\eta$ | Fractional Spanwise Co-ordinate |
| $\theta$ | Twist of Wing - positive nose up, measured in chordwise direction |
| $\xi$ | Aileron Angle, measured in chordwise direction |

## 1. INTRODUCTION

### 1.1 General

The rolling power of a flexible wing is nearly always less than that of a similar rigid wing. This loss in rolling power arises because the loads produced by a deflected aileron distort the wing in a mode giving a rolling moment in the opposite sense to that produced by the deflected aileron. Since the restraining stiffness of the wing is constant and the distorting loads applied by the deflected aileron increase with air speed, it follows that the wing twist will increase with air speed. At some speed the adverse rolling moment due to wing twist will become equal and opposite to that produced by the aileron and the net rolling power of the wing will be reduced to zero. The speed at which this occurs is known as the "aileron reversal speed".

This aileron reversal was first experienced in the 1920's and the theory of aileron reversal for straight wings was satisfactorily discussed by Pugsley (Ref.1) and others. The introduction of thin sweptback wings to delay compressibility effects at high subsonic Mach numbers has revived the problem.

Much research and study has been carried out on sweptback wings, but little data concerning aeroelastic phenomena have been released. It has been the object of the work described here to study the variations of aileron reversal speed, and rolling power in general, with the angle of sweepback of the wing. A similar study has been carried out in the United States (Ref.2) but with the emphasis on the effect of various aileron configurations on the rolling power.

### 1.2 Aerodynamic Data

Ideally, in an investigation of this nature, all the relevant aerodynamic derivative coefficients, namely $a_1$, $a_2$ and $m$, should be determined from experimental results, and the tests were in fact devised so that the values of the coefficients $a_1$ and $a_2$ could be calculated from the results. This approach allowed the variation of these coefficients with sweepback to be investigated.

The value of the coefficient $m$ could not be derived from the present tests; the value used was therefore obtained as follows. The aileron chord was in all cases one-quarter of the total chord, and for this configuration the theoretical value of $m$ for an unswept wing, namely 0.65, is nearly equal to that for $a_2/a_1$ (0.61 approximately). Moreover, simple considerations of an infinite swept wing indicate that all the coefficients are reduced below the unswept values in the ratio $\cos \gamma$ where $\gamma$ is the angle of sweep*. Accordingly, in the present work it is assumed that

$$m = (a_2/a_1) \cos \gamma .$$

### 1.3 Elastic Data

The structural aspect of the problem of aileron reversal has been considerably complicated by the introduction of sweepback.

In order to avoid confusion, the following definitions are necessary.

*See Appendix I.

### 1.3.1 Definitions

FLEXURAL CENTRE - The flexural centre of a section of a wing is defined as that point in the plane of the section at which a shear load will produce no twist of the section in that plane. It is emphasised that the position of the flexural centre depends upon the orientation of the section.

FLEXURAL AXIS - The flexural axis is defined as the locus of the flexural centres.

NORMAL SECTION - The normal section is defined to be the plane normal to the quarter chord line of the wing.

CHORDWISE SECTION - The chordwise section is defined to be the plane parallel to the direction of the airstream. N.B. The normal and chordwise sections coincide for an unswept wing.

### 1.3.2 Flexural Axis of Swept Wing

It is convenient to consider the problem in relation to a simple spar of uniform section which is built in at one end to a vertical wall (see Fig. 1). In the case of the spar which is 'straight', that is, normal to the plane of the supporting wall, the flexural axis will be the locus of the shear centres of the spar. Thus, for example, in a symmetrical rectangular box spar the flexural axis will coincide with the centroidal axis of the spar and will be parallel to the spar and normal to the plane of support. In addition any force producing a bending deflection will not produce rotation of the spar, neither will a torque produce any bending deflection (Fig. 1(a)).

On the 'swept' spar, however, the position is not so straightforward. Two approaches are possible, using either the normal or the chordwise direction as the second co-ordinate of the system.

If the normal section is used, and provided end effect is negligible, the flexural axis will be the locus of the shear centres as in the straight spar and the axis will lie along the spar (Fig. 1(b)). A vertical load at some point 'Y' on the spar will cause no twist of the normal section through Y, that is, NN'. It will, however, produce a twist of the chordwise section CC'. The main disadvantage of this approach lies in the fact that the aerodynamic loads will be computed, using strip theory, for the chordwise strips. Thus any pitching or bending moments must be resolved into the normal plane and a moment in either sense will cause both flexural and torsional deflections.

If the chordwise direction is considered, the flexural centre of a section will be at some point 'P' in front of the spar. This may readily be established by simple analysis which shows that if the spar is of uniform section, the locus of P will be a straight line as indicated in the diagram. If this convention is adopted a shear load applied at P will produce no rotation of the section CC'. There will be, in general, a small rotation at any section due to shear loads applied on the flexural centre of other sections. A brief discussion of these points is given in Appendix II.

The concept of different flexural axes according to the direction considered has been emphasised as this often a cause of confusion. The different axes may be conveniently termed the

"flexural axis of the chordwise section" and the "flexural axis of the normal section".

In this report the chordwise section has been used throughout. Since the wing spar, situated at the quarter chord, is the main structural member, the flexural axis will be observed to lie in front of the quarter chord line in all except the straight and sweptforward wings.

### 1.3.3 Stiffness of a Swept Wing

For the purposes of comparison and also to calculated the reversal speed of a wing, it is necessary to obtain the stiffness characteristics of the wing.

The use of tables of flexibility coefficients, which may be used in matrix form, is the most comprehensive way of expressing the elastic characteristics of a wing. This approach is considered in Ref. 3, but considerable time is necessary to obtain these stiffness matrices from tests and because of this they were not used in the work described here. They have the added disadvantage that they do not readily provide a single parameter of stiffness for comparison.

An alternative method is to use overall stiffnesses similar to $n_\theta$ and $l_\phi$ that is, to determine at some reference section the moments required to produce unit twist and unit bending deflection of the section.

In this paper $n_\theta$ and $l_\phi$ have been used relating to a chordwise reference section, $l_\phi$ being measured along the flexural axis of the chordwise sections. Since, with this configuration, pure bending deflections at the reference section produce only small torsional deflections elsewhere, the effect of variation of $l_\phi$ from wing to wing has been ignored.

A further alternative is presented in Ref. 4 in which the author assumes a detailed knowledge of stiffness distribution along the wing.

## 2. APPARATUS

### 2.1 Wind Tunnel

The wind tunnel testing was carried out in the 3ft 6 in. diameter, open jet, return-flow tunnel of the University of Bristol. A speed range of 40 to 130 ft per second can be achieved in the working section.

### 2.2 Pylon

In order to support the wings at the level of the centre line of the jet, a streamlined pylon was constructed. The model wings were mounted in the rear half of the "fuselage" at the top of this pylon. The rear half of the fuselage could rotate on a shaft which ran in two ball races in the front half of the fuselage (Fig. 3). In this manner it was possible to simulate free rolling conditions using a semi-span wing, suitably balanced.

In addition, a rod contained within the pylon could be screwed into a fitting attached to the shaft, thus preventing rotation of the rear half of the fuselage. The rolling moments

acting upon the rear fuselage were carried to the base of the pylon by the rod. These moments were measured with a beam balance, mounted beside the working section, and connected to the rod by a 0.010 in. steel wire (Fig. 2). A wire was used in order to reduce buffeting of the system by the turbulent air surrounding the jet. The lower end of the rod was fitted with baffle plates which, when immersed in heavy oil, provided the necessary damping for the balance system.

2.3 Model Wings (Figs. 4 and 5)

In order that the aeroelastic phenomena under discussion should be appreciable at the moderate airspeeds available, it was necessary that the model wings used should have a low torsional stiffness but that this should not be achieved at the expense of bending stiffness and general durability.

A family of six semi-span wings was constructed having the same span, aspect ratio and aerofoil section but with sweeps varying from 15° sweepforward to 60° sweepback in increments of 15°. These wings were constructed after the manner shown in Fig. 4 using conventional aeromodelling techniques involving the use of balsa wood framework, designed to have a standard stiffness, covered in doped tissue paper. The framework consisted of a tapered spar, located at the quarter chord line, which was the main structural member. The leading and trailing edges had negligible bending stiffness. Most of the torsional stiffness was derived from the covering material which was intitially treated with a minimum quantity of cellulose dope necessary to achieve a taut, airtight surface. It was then possible to produce subsequent increases in torsional stiffness by applying further coats of dope to enable tests to be carried out over a range of stiffness sufficient to eliminate the variation in stiffness from wing to wing.

The main dimensions of the wing are shown in Fig. 4.

Two solid mahogany wings were also constructed to obtain comparative rigid wing results.

All the wings had a standard tongue root fitting which enabled them to be interchanged in the fuselage on the pylon.

2.4 Structural Test Apparatus

A contour board was constructed which could be attached to the wing by clamping screws at the leading and trailing edges. Graduated scales on the contour board above the leading and trailing edges of the wing were then observed through a pair of telescopes. A series of holes was provided along the bottom edge of the contour board so that shear loads could be applied at various chordwise stations on the wing.

3. THEORY

Throughout the structural testing the chordwise co-ordinate system was used, and for consistency the aerodynamic loads are considered acting upon a chordwise strip of the wing.

The use of the chordwise co-ordinate system has the advantage that a family of wings may be defined having the same span, aspect ratio and chordwise aerofoil section and varying only in the amount of sweep.

The effect of sweepback is then introduced into the theory as variation of the position of the flexural axis of the chordwise sections and of the aerodynamic coefficients.

The position of the flexural axis was derived from the structural tests (see Section 4.1) and the values of the aerodynamic coefficients, obtained as $a_2$ and $a_2/a_1$ for the chordwise section, were calculated from the rolling moment and rolling velocity tests respectively. As in the theory for calculated reversal speeds, Strip Theory was used and it was assumed that the coefficients for each wing were independent of the spanwise co-ordinate.

As already indicated, the approximation

$$n = (a_2/a_1) \cos \gamma$$

is used for all the wings considered.

The further assumption has been made that the flexural axis of the model wings is a straight line, passing through the quarter chord point at the root. Tests on the 30° wing showed that this assumption was justified for the structural configuration used in the models.

The rolling moment produced by a flexible wing under general conditions can be written

$$R = q \int_a a_2 \xi c y dy - q \int_w a_1 \frac{py}{V} c y dy + q \int_w a_1 \theta c y dy$$

where the suffixes w and a imply integration over the wing and aileron respectively.

For a wing of constant chord and assuming that

(i) aerodynamic coefficients $a_1$, $a_2$ and n are independent of span

(ii) aileron angle is constant,

we have, writing $y = \eta s$ and assuming the aileron extends from $y = \eta_1 s$ to $y = \eta_2 s$,

$$\frac{R}{q\xi} = a_2 s^2 \int_a c\eta d\eta - a_1 \frac{ps}{\xi V} s^2 \int_w c\eta^2 d\eta + a_1 s^2 \int_w c\eta \frac{\theta}{\xi} d\eta, \qquad \ldots(1)$$

where the suffix a now implies the limits $\eta_1$ to $\eta_2$, and w implies 0 to 1: strictly the lower limit for w should correspond to the "fuselage" radius, but since the integrands all vanish at $\eta = 0$, there is little error in taking the lower limit to be zero.

Writing $R = C_l q Ss = C_l q \bar{c} s^2$ where $\bar{c}$ is the mean chord, we have

$$\frac{C_l}{\xi} = a_2 \int_a \frac{c}{\bar{c}} \eta d\eta - a_1 \frac{ps}{\xi V} \int_w \frac{c}{\bar{c}} \eta^2 d\eta + a_1 \int_w \eta \frac{c}{\bar{c}} \frac{\theta}{\xi} d\eta \qquad \ldots(2)$$

Tests were carried out under two conditions, namely,

(i) $R = 0$. This corresponds to steady rolling conditions.

(ii) $p = 0$. This corresponds to conditions applying immediately the aileron is deflected and before rolling commences.

These two conditions apply simultaneously at reversal.

Considering condition (i) from equation (1) if $R = 0$:

$$\frac{ps}{\xi V}\int_w \frac{c}{\bar{c}}\eta^2 d\eta = \frac{a_2}{a_1}\int_a \frac{c}{\bar{c}}\eta d\eta + \int_w \frac{c}{\bar{c}}\frac{\theta}{\xi}\eta d\eta \qquad \ldots(3)$$

and from condition (ii)

$$\frac{C_l}{\xi} = a_2\int_a \frac{c}{\bar{c}}\eta d\eta + a_1\int_w \frac{c}{\bar{c}}\frac{\theta}{\xi}\eta d\eta \qquad \ldots(4)$$

Equations (3) and (4) were used to evaluate the coefficients $a_1$ and $a_2$ by considering the limiting experimental values of $ps/\xi V$ and $C_l/\xi$ as $V$ tends to zero, that is, as the twist, $\theta$, tends to zero. These limiting cases of rolling power correspond to the rigid wing cases. Typical curves are given in Figs. 6 and 7.

Equations (3) and (4) cannot, in general, be solved for any finite speed because the form of $\theta$ is unknown. There are two methods of approach depending on the amount of structural data available. If it is possible to obtain the stiffness distribution in the form of flexibility coefficients an iterative process of solution may be applied; this will give the rolling power and mode of twist at any speed. This method is set out in Ref. 3.

The alternative approach is that of semi-rigidity in which a suitable mode of distortion is assumed (Ref. 1), which enables equations (3) and (4) to be solved. It is emphasised that the solutions obtained depend acutely on the accuracy of the mode assumed; moreover, the correct mode will, in general, vary with speed.

With the latter approach, and with $\theta = \theta_r f(\eta)$ where $f$ is the spanwise distribution of twist, equation (2) becomes

$$\frac{C_l}{\xi} = a_2\int_a \frac{c}{\bar{c}}\eta d\eta - a_1\frac{ps}{\xi V}\int_w \frac{c}{\bar{c}}\eta^2 d\eta + \frac{\theta_r}{\xi}a_1\int_w \frac{c}{\bar{c}}\eta f d\eta \qquad \ldots(5)$$

where $\theta_r$ is the twist at the reference section $\eta_r$ and $f(\eta_r) = 1$. A further expression for $\theta_r/\xi$ may be derived from considering the torsional equilibrium of a section of the wing, whence:-

$$\frac{\theta_r}{\xi}\left(\frac{I_\theta}{q} - a_1 s\int_w ec^2 f^2 d\eta\right) = s\int_a c^2(ea_2 - m) f d\eta - \frac{ps}{\xi V}a_1 s\int_w ec^2 f\eta d\eta \qquad \ldots(6)$$

where $ec$ is the distance of the flexural axis aft of the aerodynamic centre. For the wings considered in this paper it was found that the position of the flexural axis could be expressed as

$$e = \frac{sT\eta}{c}$$

where $T$ is a constant depending only on sweep and stiffness.

Substituting for $e$ in equation (6) we have

$$\frac{\theta_r}{\xi}\left[\frac{n_\theta}{q} - a_1 s^2 T\bar{c}\int_0^1 \frac{c}{\bar{c}} f^2\eta d\eta\right] = a_2\bar{c}s^2T\int_{\eta_1}^{\eta_2}\frac{c}{\bar{c}} f\eta d\eta - n\bar{c}^2 s\int_{\eta_1}^{\eta_2}\left(\frac{c}{\bar{c}}\right)^2 f d\eta$$

$$- \frac{ps}{\xi V} a_1 s^2\bar{c}T\int_0^1 \frac{c}{\bar{c}} f\eta^2 d\eta \qquad \ldots(7)$$

If we define

$$\left.\begin{aligned}
A &= a_1 s^2 T\bar{c}\int_0^1 \frac{c}{\bar{c}} f^2\eta d\eta \\
B &= a_1\int_0^1 \frac{c}{\bar{c}}\eta f d\eta \\
C &= a_2\int_{\eta_1}^{\eta_2}\frac{c}{\bar{c}}\eta d\eta \\
D &= a_1\int_0^1 \frac{c}{\bar{c}}\eta^2 d\eta \\
E &= a_2\bar{c}s^2T\int_{\eta_1}^{\eta_2}\frac{c}{\bar{c}} f\eta d\eta \\
F &= n\bar{c}^2 s\int_{\eta_1}^{\eta_2}\left(\frac{c}{\bar{c}}\right)^2 f d\eta \\
G &= a_1 s^2\bar{c}T\int_0^1\left(\frac{c}{\bar{c}}\right) f\eta^2 d\eta
\end{aligned}\right\} \qquad \ldots(8)$$

then equation (7) becomes

$$\frac{\theta_r}{\xi}\left[\frac{n_\theta}{q} - A\right] = E - F - \frac{ps}{\xi V}(G) \qquad \ldots(9)$$

Considering the two conditions of reversal, and substituting from (8) and (9) in (5) to eliminate $\theta_r$, we have

(i) when $R = 0$, i.e., $C_l = 0$,

$$\frac{ps}{\xi V}\left[D + \frac{BG}{\left(\frac{n_\theta}{q} - A\right)}\right] = C + \frac{B(E-F)}{\left(\frac{n_\theta}{q} - A\right)} \qquad \ldots(10)$$

(ii) when $p = 0$

$$\frac{C_l}{\xi} = C + \frac{B(E - F)}{\left(\frac{n_\theta}{q} - A\right)} \qquad \ldots(11)$$

It will be noted that equations (10) and (11), when applied to the reversal conditions, yield

$$q_r = \frac{n_\theta C}{AC - B(E - F)} \qquad \ldots(12)$$

Apart from variations in T, equation (12) shows that for a particular angle of sweep $q_r$ is proportional to $n_\theta$.

Equations(12) was solved using a mode of the form

$$f = A \sin \frac{\pi\eta}{2},$$

which was found to be very nearly the actual distortion mode at reversal, to estimate the reversal speeds of the model wings.

## 4. TEST PROCEDURE

### 4.1 Structural Tests

Each wing was tested at three different stiffnesses so that, by interpolation, the results could be compared at a common stiffness.

The torsional stiffness was found in the usual way by loading a contour board situated on the wing at the reference section and lying in a plane containing the wind direction. From the twist at the reference section for given loads the torsional stiffness, $n_\theta$ and the position of the flexural axis were determined.

The unusual position of the reference section ($\eta = 0.892$) was chosen to enable the results to be used to form stiffness matrices; these were not, however, completed.

### 4.2 Rolling Velocity Tests

Initially when each wing was mounted in the fuselage the aileron was set in its neutral position and the incidence of the whole wing adjusted until there was no tendency to roll at any airspeed. Aileron angles were set manually and retained by fixing strips of celluloso tape, one on each side of the wing-aileron gap. These also served to seal the gap against air leakage.

The aileron was deflected a measured amount and the rate of roll observed at a series of airspeeds up to the point at which the wing would remain stationary at one of several positions around its rolling path. This procedure was repeated for a range of aileron angles, generally about six in all, varying from -15° to +15°.

### 4.3 Rolling Moment Tests

After each wing had been tested under steady rolling conditions the rod within the pylon was locked into the fuselage pivot shaft so that the wing was horizontal. In order that rolling moments of both senses could be measured, an external balance weight was added opposite the wing, to keep the wire connecting the rod and the balance in tension at all times.

The rolling moment produced by the wing was then observed over a range of airspeed, up to the reversal speed, for each of a series of aileron angles ranging from -15° to +15° in 5° increments.

### 4.4 Measurement of Deflected Form of Wing at Reversal

A pair of photographs was taken of the 30° wing, fixed in a horizontal position, one exposure being taken at zero airspeed and the other at the reversal speed of the wing. The photographs were taken along a line normal to the leading edge of the wing and the double image on the plate was examined under a travelling microscope to determine the modes of distortion.

## 5. PRESENTATION OF RESULTS

The results obtained during the experiments are summarised in in the Tables.

The structural characteristics of the wings are shown in Table I, while Tables II and III show the rolling power of each wing expressed as the helix angle in roll for a unit aileron deflection in the case of the rolling velocity tests, and as the rolling moment coefficient for a unit aileron deflection for rolling moment tests. Representative curves for these tables are shown in Figs. 6 and 7. These results have been reduced to those for a common stiffness and are shown in Fig. 8 for the helix angle in roll.

The values of the aerodynamic coefficients, deduced as indicated in §3 from the test results, together with the assumed values of $n$, are shown in Fig. 9.

The variation of the reversal speed of the wing (at the common stiffness) with sweep is shown in Fig. 10, together with the predicted values of reversal speeds obtained from the semi-rigid theory.

## 6. DISCUSSION OF RESULTS

### 6.1 General

The results indicate that the rolling power of the wings decreases with increase of speed in a roughly parabolic manner, the introduction of sweepback producing no basic change in the shape of the curve. The curves become flatter as sweepback is increased since the peak rolling power decreases steadily with the decrease of the aerodynamic coefficients.

The values of the aerodynamic coefficients plotted in Fig. 9 are those for the flexible wings. It will be noted that the values for the solid wings are appreciably higher than those for the flexible wings, as was expected, since the construction of the flexible wings made it impossible to maintain the exact aerofoil section. In all cases the value of $a_1$ was considerably lower than was expected. This may have been due to the low Reynolds number of the tests ($0.3 \times 10^6$ at the maximum test speed).

### 6.2 Correlation of Rolling Velocity and Rolling Moment Tests

It will be seen that in general the reversal speed as measured by the rolling velocity tests is lower than that measured in the rolling moment tests. This is felt to be probably due to misalignment of the pylon. If the pylon is not exactly in line with the windstream, or if there are any local flow disturbances, it is possible for the wing to stop rolling prematurely, hence giving a false value of the reversal

speed. This effect is characterised by the wing stopping in the same angular position on each occasion. The alignment of the pylon was frequently checked to eliminate this error as far as possible and its effect was therefore minimised.

It is felt that in view of this the reversal speed as measured by the rolling moment tests is the more reliable.

A larger discrepancy than usual between the two values of reversal speed is noticed for the straight and sweptforward wings. This is probably due to the fact that the wake from the pylon has a disturbing influence on the wings when rolling and this influence will be considerably more pronounced for the wings which pass close to the pylon.

6.3 Order of Errors

In practice it was found that it was possible to set the incidence of the wing by the method described at the beginning of §4.2 to a degree of accuracy corresponding to an error in the aileron setting of 0.4° approximately. The accuracy with which it was possible to set the aileron deflections themselves was of the order of $\pm 0.2°$.

These errors were minimised in the analysis of tests results by cross-plotting rolling power at various speeds against aileron deflection.

The errors involved in obtaining wing stiffness were also minimised by cross-plotting, but it is felt that some errors were unavoidable as the wings were slightly affected by humidity, etc.

6.4 Comparison with Theory

It will be seen from Fig. 10 that the predicted reversal speeds show good correlation with the experimental results except at very high angles of sweepback. The discrepancy in the case of the wing with 60° sweepback is felt to be due partially to the difficulty in obtaining consistent results with that particular wing. It is also likely that the assumed value of $n$ is in error at high angles of sweep.

## 7. CONCLUSIONS

The test results indicate that, in the absence of compressibility effects, the reversal speed of swept wings will increase with the increase of both sweep forward and sweepback, the minimum reversal speed occurring at approximately 15° sweepback. The results for the 60° wing are open to some question as the stiffness characteristics of this wing differed widely from the rest of the family.

Due to the decrease of the aerodynamic coefficients $a_1$ and $a_2$ with sweepback, the rolling power of the wings at low speeds shows a steady decrease, the value for the wing with 60° sweepback being less than half the value obtained for the straight wing at the same stiffness.

The value of the dynamic head at reversal was found to be very nearly proportional to the stiffness as measured by $n_\theta$ at the reference section for a particular wing, as the theory indicates (§3. Equation (12)).

The twist mode at reversal of the 30° sweptback wing was found to be nearly sinusoidal and the adoption of this mode in analysis based on semi-rigid theory gives theoretical reversal speeds which, on the whole, agree very well with experimental results. It would therefore appear that the semi-rigid hypothesis is adequate when used over a limited range of sweep for which the variation of the aerodynamic coefficients can be accurately established.

## 8. REFERENCES


1. Pugsley, A. G. — The Aerodynamic Characteristics of a Semi-rigid Wing, Relevant to the Problem of Loss of Lateral Control due to Wing Twisting. R. & M. 1490, June, 1932. See also R. & M. 1506, 1508, 1640, etc.

2. Cole, H. A. C.; Ganzer, V. M. — Experimental Investigation of Rolling Performance of Straight and Sweptback Flexible Wings with Various Ailerons. N.A.C.A. Technical Note 2563, December, 1951.

3. Broadbent, E. G. — Rolling Power of an Elastic Swept Wing. R. & M. 2857. July, 1950.

4. Templeton, H. — Control Reversal Effects on Sweptback Wings. Aeronautical Quarterly, Vol. I, May, 1949.

TABLE I

Structural Characteristics of Wings

| WING (Angle of Sweepback) | CONDITION | $m_\theta$ lb ft/rad | $l_\phi$ lb ft/rad | T |
|---|---|---|---|---|
| -15° | 1st Stiffness | 1.77 | 9.89 | +0.0832 |
| | 2nd Stiffness | 2.09 | 9.96 | +0.0944 |
| | 3rd Stiffness | 2.29 | 10.46 | +0.0976 |
| Straight | 1st Stiffness | 1.45 | 13.38 | -0.0024 |
| | 2nd Stiffness | 1.58 | 14.80 | +0.0040 |
| | 3rd Stiffness | 1.91 | 15.90 | +0.0112 |
| 15° | 1st Stiffness | 1.42 | 9.35 | -0.0400 |
| | 2nd Stiffness | 1.88 | 9.35 | -0.0648 |
| | 3rd Stiffness | 2.02 | 10.22 | -0.0696 |
| 30° | 1st Stiffness | 1.73 | 12.60 | -0.1216 |
| | 2nd Stiffness | 1.97 | 12.54 | -0.1264 |
| | 3rd Stiffness | 2.13 | 12.90 | -0.1192 |
| 45° | 1st Stiffness | 1.31 | 13.41 | -0.1120 |
| | 2nd Stiffness | 1.75 | 13.73 | -0.1432 |
| | 3rd Stiffness | 1.80 | 13.80 | -0.1568 |
| 60° | 1st Stiffness | 1.13 | 7.97 | -0.1520 |
| | 2nd Stiffness | 1.32 | 8.47 | -0.2776 |
| | 3rd Stiffness | 1.50 | 9.55 | -0.3072 |

T is defined in Section 4 and is positive if the flexural axis is behind the quarter chord line.

## TABLE II

Values of Helix Angle in Roll - $\frac{p_s}{\xi V}$

| q - lb/ft² | | 0 | 2.15 | 4.30 | 6.45 | 8.60 | 9.68 | 10.75 | 11.83 | 12.9 | 13.99 | 15.05 | 16.13 | 17.20 | | |
|---|---|---|---|---|---|---|---|---|---|---|---|---|---|---|---|---|
| V - ft/sec | | 0 | 42.5 | 60.2 | 73.6 | 85.0 | 90.4 | 95.1 | 99.6 | 104.0 | 108.5 | 112.7 | 116.7 | 120.4 | | |
| | $n_\theta$ | | | | | | | | | | | | | | $V_r$ | $q_r$ |
| $\overline{15}$ | 1.77 | .619 | .576 | .490 | .392 | .256 | .175 | .111 | .041 | | | | | | 102.0 | 12.20 |
| | 2.09 | .600 | .578 | .529 | .461 | .379 | .332 | .279 | .228 | .175 | .121 | .0735 | | | 117.7 | 16.33 |
| | 2.29 | .576 | .567 | .531 | .475 | .400 | .356 | .318 | .262 | .214 | .153 | .1017 | .0480 | | 119.6 | 17.10 |
| 0 | 1.45 | .594 | | .490 | .374 | .210 | .111 | .0175 | | | | | | | 95.8 | 10.92 |
| | 1.58 | .604 | .572 | .498 | .378 | .248 | .173 | .090 | | | | | | | 99.7 | 11.80 |
| | 1.91 | .574 | .565 | .505 | .434 | .340 | .286 | .224 | .166 | .102 | .036 | | | | 110.8 | 14.60 |
| 15 | 1.42 | .567 | .512 | .420 | .313 | .206 | .140 | .0875 | .0350 | | | | | | 102.1 | 12.40 |
| | 1.88 | ----------D O P E D--------I N--------E R R O R---------- | | | | | | | | | | | | | ----- | ----- |
| | 2.02 | .567 | .526 | .470 | .394 | .312 | .262 | .212 | .164 | .1155 | .061 | | | | 112.9 | 15.20 |
| 30 | 1.73 | .485 | .467 | .425 | .350 | .257 | .206 | .156 | .105 | .054 | | | | | 108.8 | 14.0 |
| | 1.97 | .510 | .493 | .453 | .397 | .318 | .282 | .250 | .200 | .148 | .090 | | | | 115.0 | 15.75 |
| | 2.13 | .493 | .464 | .424 | .372 | .310 | .273 | .236 | .200 | .161 | .119 | .075 | .033 | | 119.8 | 17.0 |
| 45 | 1.31 | .457 | .445 | .410 | .330 | .2095 | .1365 | .0817 | | | | | | | 99.1 | 11.70 |
| | 1.75 | .326 | .362 | .378 | .321 | .259 | .224 | .193 | .152 | .109 | .067 | .031 | | | 115.3 | 15.80 |
| | 1.80 | .338 | .397 | .404 | .371 | .324 | | .248 | .203 | .167 | .121 | .076 | .029 | | 118.9 | 16.80 |
| 60 | 1.13 | .222 | .245 | .278 | .237 | .191 | .149 | .130 | | | | | | | 113.1 | 15.20 |
| | 1.32 | .249 | .260 | .258 | .230 | .203 | .170 | .148 | .120 | .083 | .054 | .025 | | | 115.0 | 15.74 |
| | 1.50 | .259 | .284 | .303 | .293 | .253 | .237 | .212 | .188 | .169 | .137 | .106 | .074 | .034 | 123.6 | 18.21 |

## TABLE III

### Values of Rolling Moment Coefficient $\frac{C_l}{\xi}$

| q - lb/ft² | | 0 | 2.15 | 4.30 | 6.45 | 8.60 | 9.68 | 10.75 | 11.83 | 12.90 | 13.99 | 15.05 | 16.13 | 17.20 | | |
|---|---|---|---|---|---|---|---|---|---|---|---|---|---|---|---|---|
| V - ft/sec | | 0 | 42.5 | 60.2 | 73.6 | 85.0 | 90.4 | 95.1 | 99.6 | 104.0 | 108.5 | 112.7 | 116.7 | 120.4 | | |
| | $\mu_\theta$ | | | | | | | | | | | | | | $V_r$ | $q_r$ |
| $\overline{15}$ | 1.77 | .2810 | .2750 | .2492 | .2310 | .1892 | .1654 | .1480 | | | | | | | 111.8 | 14.80 |
| | 2.09 | .2910 | .2830 | .2050 | .2312 | .1790 | | .1300 | .1091 | .0889 | .0662 | .0480 | | | 133.1 | 21.05 |
| | 2.29 | .2780 | .2751 | .2632 | .2479 | .2381 | .2302 | .2170 | .2050 | .1860 | .1640 | .1380 | | | 156.8 | 29.25 |
| 0 | 1.45 | .3080 | .2596 | .2092 | .1559 | .1080 | | | | | | | | | 105.0 | 13.11 |
| | 1.58 | .2840 | .2742 | .2476 | .2110 | .1598 | .1363 | .1046 | .0797 | .0519 | | | | | 111.2 | 14.69 |
| | 1.91 | .3000 | .2818 | .2508 | .2122 | .1697 | .1455 | .1093 | .0990 | .0727 | .0490 | .0246 | | | 116.8 | 16.17 |
| 15 | 1.42 | .2138 | .2048 | .1741 | .1277 | .0616 | .0398 | | | | | | | | 95.1 | 10.75 |
| | 1.88 | .2205 | . | .1827 | .1426 | .1061 | .0910 | .0702 | .0503 | .0351 | .0175 | | | | 112.0 | 14.89 |
| | 2.02 | .2080 | .1980 | .1731 | .1380 | .1073 | .0902 | .0692 | .0570 | .0393 | .0280 | | | | 114.2 | 15.51 |
| 30 | 1.73 | .2700 | .2022 | .1582 | .1249 | .0945 | .0770 | .0607 | .0442 | .0320 | | | | | 112.2 | 14.98 |
| | 1.97 | .2030 | .1855 | .1602 | .1353 | .1064 | .0930 | .0785 | .0622 | .0466 | .0354 | .0188 | | | 117.2 | 16.32 |
| | 2.13 | .1960 | .1782 | .1577 | .1314 | .1043 | .0904 | .0761 | .0600 | .0528 | .0392 | .0283 | | | 120.2 | 17.19 |
| 45 | 1.31 | .1940 | .1785 | .1492 | .1102 | .0950 | .0578 | .0386 | .0282 | | | | | | 106.2 | 13.40 |
| | 1.75 | .1890 | .1692 | .1526 | .1167 | .0905 | .0769 | .0641 | .0506 | .0365 | .0249 | | | | 115.6 | 15.87 |
| | 1.80 | .1695 | .1548 | .1360 | .1150 | .0930 | .0816 | .0717 | .0564 | .0451 | .0332 | .0282 | | | 122.0 | 17.67 |
| 60 | 1.13 | .0870 | .0653 | .0498 | .0390 | .0267 | .0226 | .0198 | | | | | | | 113.2 | 15.26 |
| | 1.32 | .0610 | .0554 | .0513 | .0429 | .0348 | .0298 | .0249 | .0201 | .0157 | .0119 | | | | 117.9 | 16.50 |
| | 1.50 | .0720 | .0659 | .0542 | .0463 | .0374 | .0338 | .0296 | .0251 | .0215 | .0174 | .0141 | .0105 | .0071 | 126.0 | 18.90 |

## APPENDIX I

### The Aerodynamic Coefficients for an Infinite Swept Wing

If the wing is assumed infinite in extent, then the velocity $W$ may be resolved into $V$ normal to the wing and $v$ parallel to the wing. $v$ has no effect on the aerodynamic forces acting on the wing.

It is assumed that there is no spanwise variation of coefficients and hence the lift on the small chordwise and normal strips of the same area will be the same.

Ignoring the velocity parallel to the wing, we have that the lift $L$ is given by

$$L = \tfrac{1}{2}\rho V^2 S(a_1 \alpha + a_2 \xi) \qquad \ldots(1)$$

where $a_1$, $a_2$ etc., are values for a straight wing, and by definition for the swept wing

$$L_S = \tfrac{1}{2}\rho W^2 S_S(a_{1S}\alpha_S + a_{2S}\xi_S) \qquad \ldots(2)$$

Now $L = L_S$; $V = W \cos \gamma$; $\alpha_S = \alpha \cos \gamma$; $\xi_S = \xi \cos \gamma$; $S_S = S$. Hence by equating equations (1) and (2)

$$\left.\begin{aligned} a_{1S} &= a_1 \cos \gamma \\ a_{2S} &= a_2 \cos \gamma \end{aligned}\right\} \qquad \ldots(3)$$

Similarly for pitching moments

$$M = \tfrac{1}{2}\rho V^2 Sc\,[ea_1\alpha + (ea_2 - m)\xi] \qquad \ldots(4)$$

and

$$M_S = \tfrac{1}{2}\rho W^2 S_S c_S\,[e_S a_{1S}\alpha_S + (e_S a_{2S} - m_S)\xi_S] \qquad \ldots(5)$$

In addition to the equalities noted above

$$M_S = M \sec \gamma; \quad c_S = c \sec \gamma; \quad \text{and} \quad e_S = e .$$

Thus from equations (4) and (5)

$$\tfrac{1}{2}\rho W^2 \cos \gamma\, Sc[ea_1\alpha + (ea_2 - m)\xi] = \tfrac{1}{2}\rho W^2 Sc \sec \gamma[ea_1\alpha \cos^2\gamma + (ea_2 \cos \gamma - m_S)\xi \cos \gamma]$$

from which it follows that

$$m_S = m \cos \gamma . \qquad \ldots(6)$$

## APPENDIX II

### Flexural Axis of a 'Swept' Spar

Consider a swept spar (Fig. 1b) whose bending stiffness (B) and torsional stiffness (C) are constant along the span. Both stiffnesses are measured along the spar.

Let x be the ordinate along the centre line of the spar and let the distance of any point from the spar be z, measured in the chordwise direction. Bending displacements are measured by y. Y is some point in the spar distant $x_1$ from the root, and P is some point on the chordwise section through Y; the ribs are assumed parallel to the chordwise direction.

Let a vertical load F be applied at P, and let PY = $z_1$. Then the moments acting will be

(a) $Fz_1 \cos \gamma$ in the plane NN'

(b) $Fz_1 \sin \gamma$ in the plane of the spar.

For torsional equilibrium in the plane normal to the spar

$$\frac{Fz_1 \cos \gamma}{C} = \frac{d\beta}{dx}$$

or

$$\beta = \frac{Fz_1 x \cos \gamma}{C} .$$

Similarly for the bending of the spar

$$\frac{Bd^2y}{dx^2} = F(x_1 - x) - Fz_1 \sin \gamma ,$$

whence

$$\frac{dy}{dx} = \frac{Fx}{2B} \cdot (2x_1 - x - 2z_1 \sin \gamma)$$

The twist at a general section, $\theta$, is thus given by

$$\theta = \beta \cos \gamma - \left( \frac{dy}{dx} \right) \sin \gamma$$

$$= Fx \left[ \frac{z_1 \cos^2 \gamma}{C} + \frac{2z_1 \sin^2 \gamma - 2x_1 \sin \gamma + x \sin \gamma}{2B} \right] \quad \ldots(1)$$

In particular the twist $\theta_1$ at $x = x_1$ is

$$\theta_1 = Fx_1 \left[ \frac{z_1 \cos^2 y}{C} + \frac{2z_1 \sin^2 y - x_1 \sin y}{2B} \right];$$

and if now $z_1$ is regarded as defining the flexural centre, so that $\theta_1 = 0$, we have

$$0 = 2B\, z_1 \cos^2 y + 2C\, z_1 \sin^2 y - Cx_1 \sin y$$

or

$$z_1 = \frac{Cx_1 \sin y}{2(B \cos^2 y + C \sin^2 y)} \qquad \ldots(2)$$

so that the flexural axis, that is, the locus of flexural centres, is a straight line.

With $z_1$ defined by (2) the general twist (1) becomes

$$\theta = \frac{F \sin y}{2B} \cdot x(x - x_1) \qquad \ldots(3)$$

that is, there is a parabolic distribution of twist, with a maximum midway between the root and loaded section. To compare this with the twist under different loading, let us imagine the load F to be applied, for example, on the spar: then the twist is given by (1) with $z_1 = 0$ and is

$$\theta = \frac{F \sin y}{2B} x(x - 2x_1) \qquad \ldots(4)$$

which is again parabolic but with its maximum at the loaded section. This maximum is four times that given by (3); accordingly, we may regard the twists given by (3) as small, though they are in general not negligible.

FIG. 1.

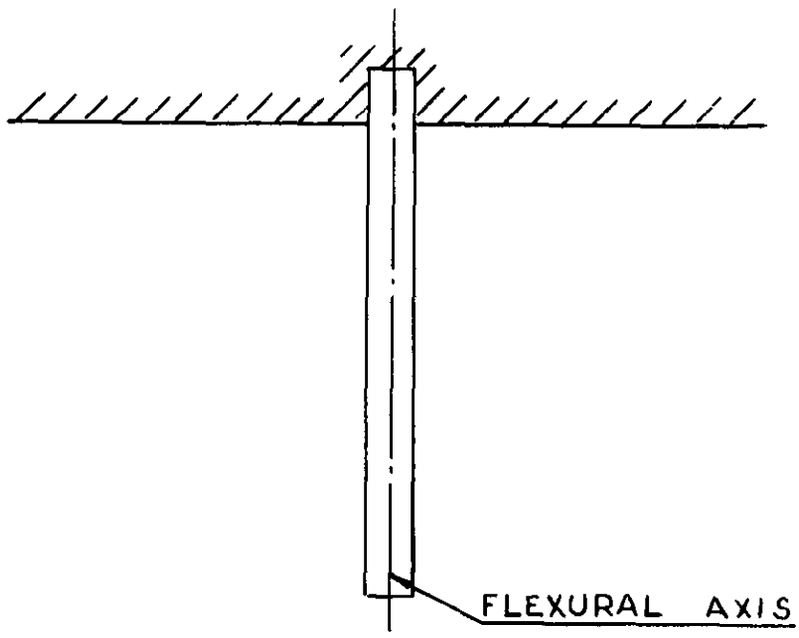


(a) 'STRAIGHT' SPAR

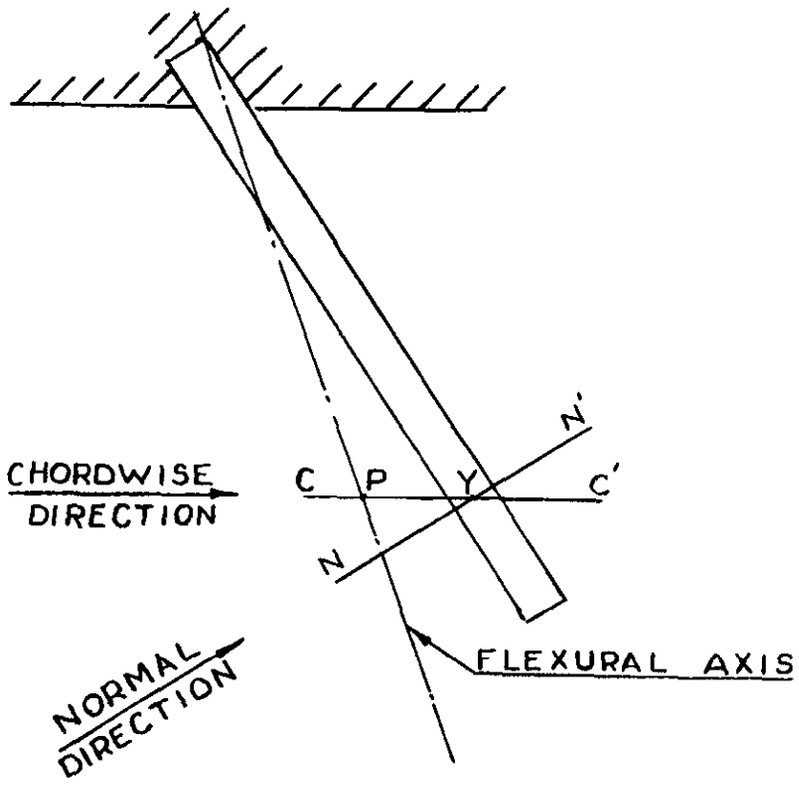


(b) 'SWEPT' SPAR

16154

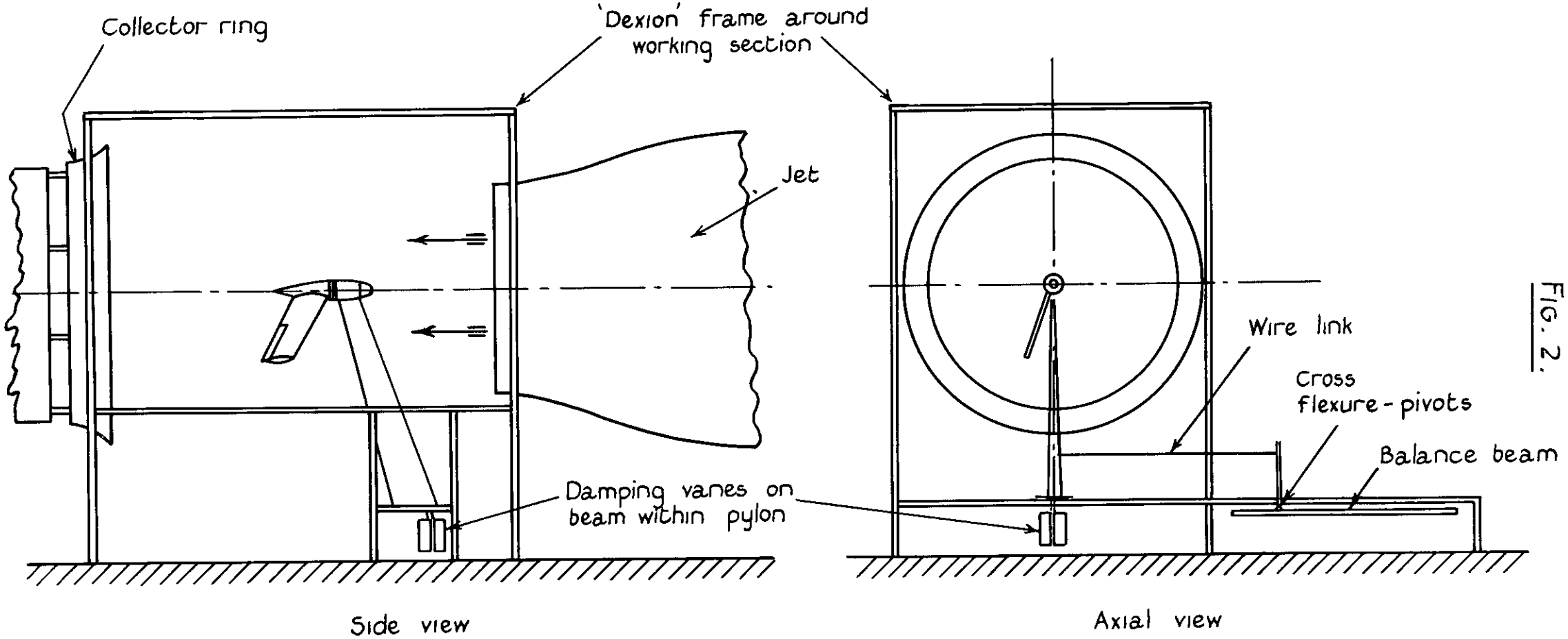


FIG. 2.

General arrangement of test apparatus

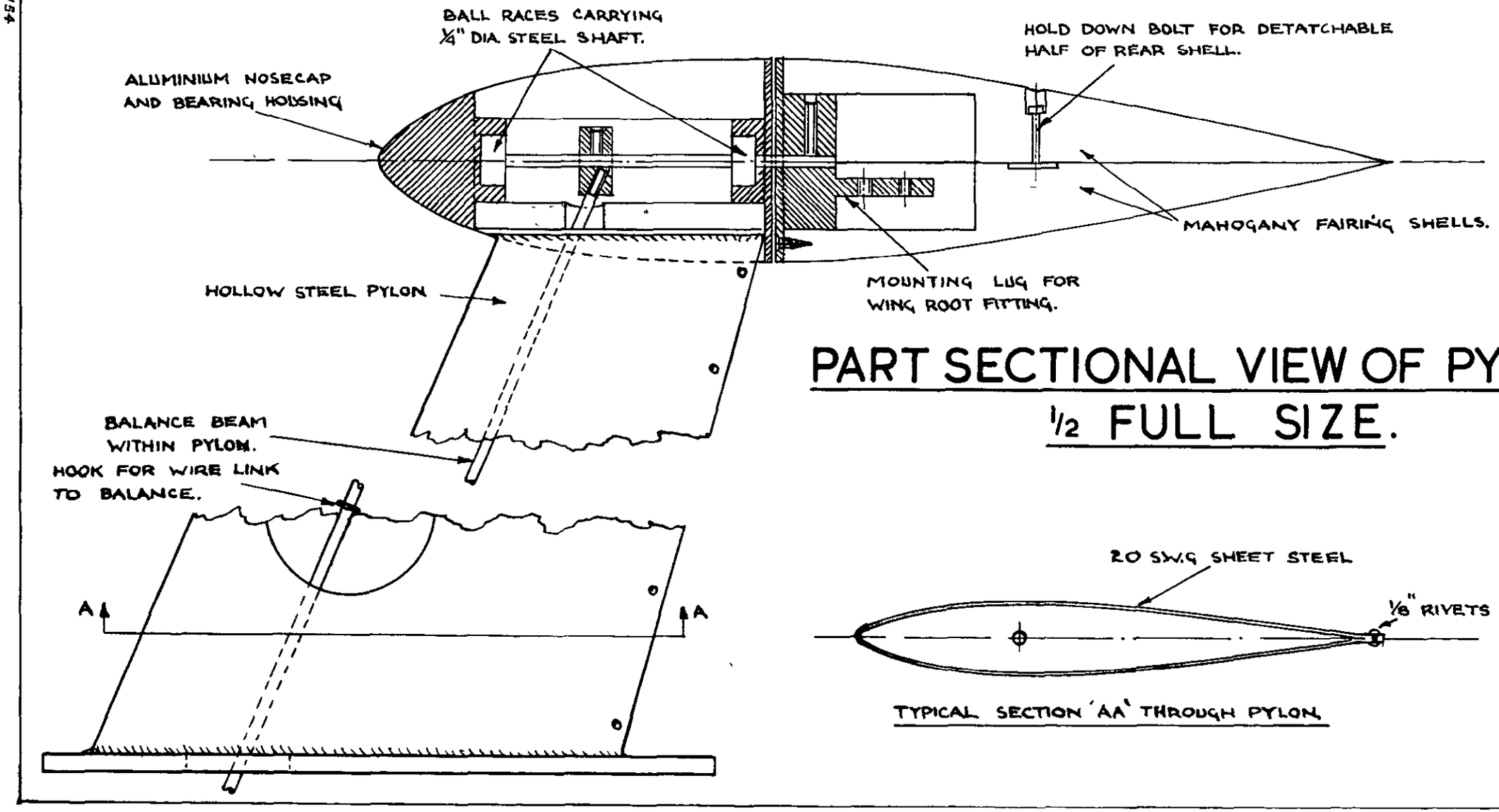


# PART SECTIONAL VIEW OF PYLON.
## ½ FULL SIZE.




TYPICAL SECTION 'AA' THROUGH PYLON.

FIG. 3

# ARRANGEMENT DRAWING OF TYPICAL WING.

1/2 FULL SIZE.

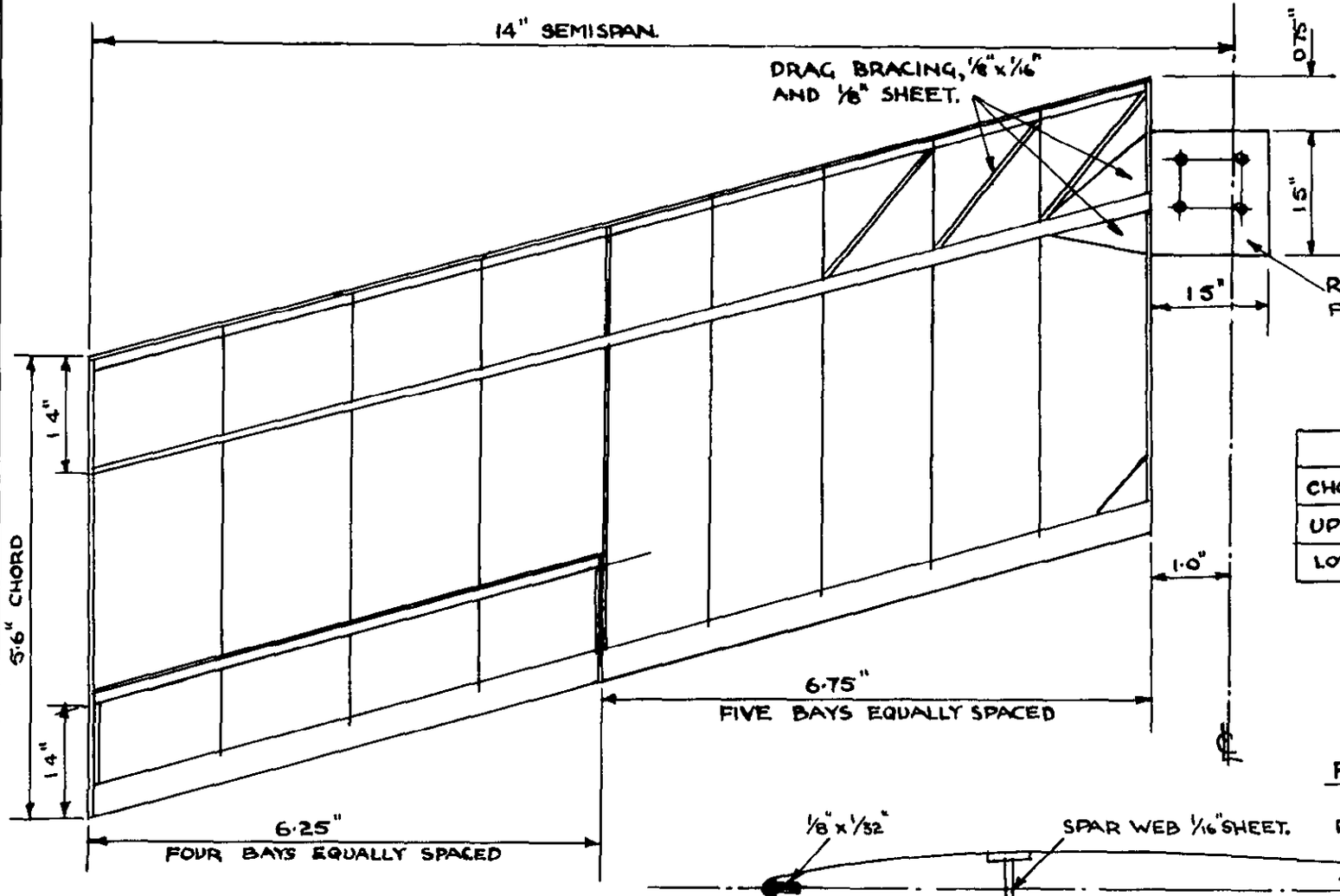


| SECTION ORDINATES (80% E 9 1040) | | | | | | | | | | | | |
|---|---|---|---|---|---|---|---|---|---|---|---|---|
| CHORD % | 0 | 5 | 10 | 20 | 30 | 40 | 50 | 60 | 70 | 80 | 90 | 100 |
| UPPER | 0 | 1.93 | 2.65 | 3.48 | 3.82 | 4.00 | 3.88 | 3.45 | 2.77 | 1.94 | 0.98 | 0 |
| LOWER | 0 | 1.93 | 2.65 | 3.48 | 3.82 | 4.00 | 3.88 | 3.45 | 2.77 | 1.94 | 0.98 | 0 |

FULL SIZE AEROFOIL SECTION

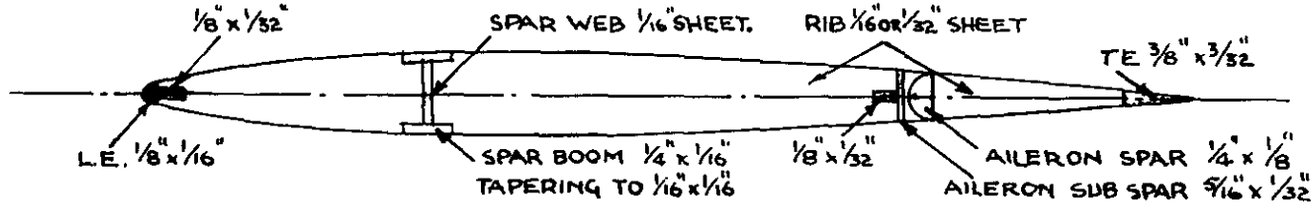


FIG. 4.

FIG 5



FAMILY OF FLEXIBLE AND SOLID MODEL WINGS.

16154

FIG. 6.

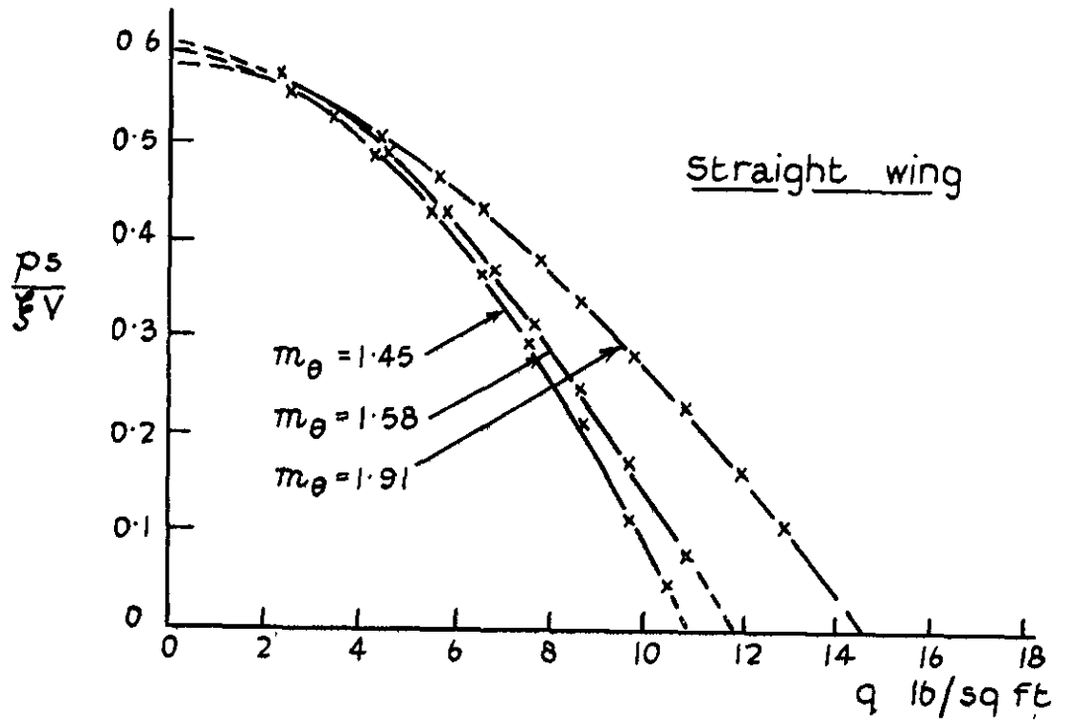


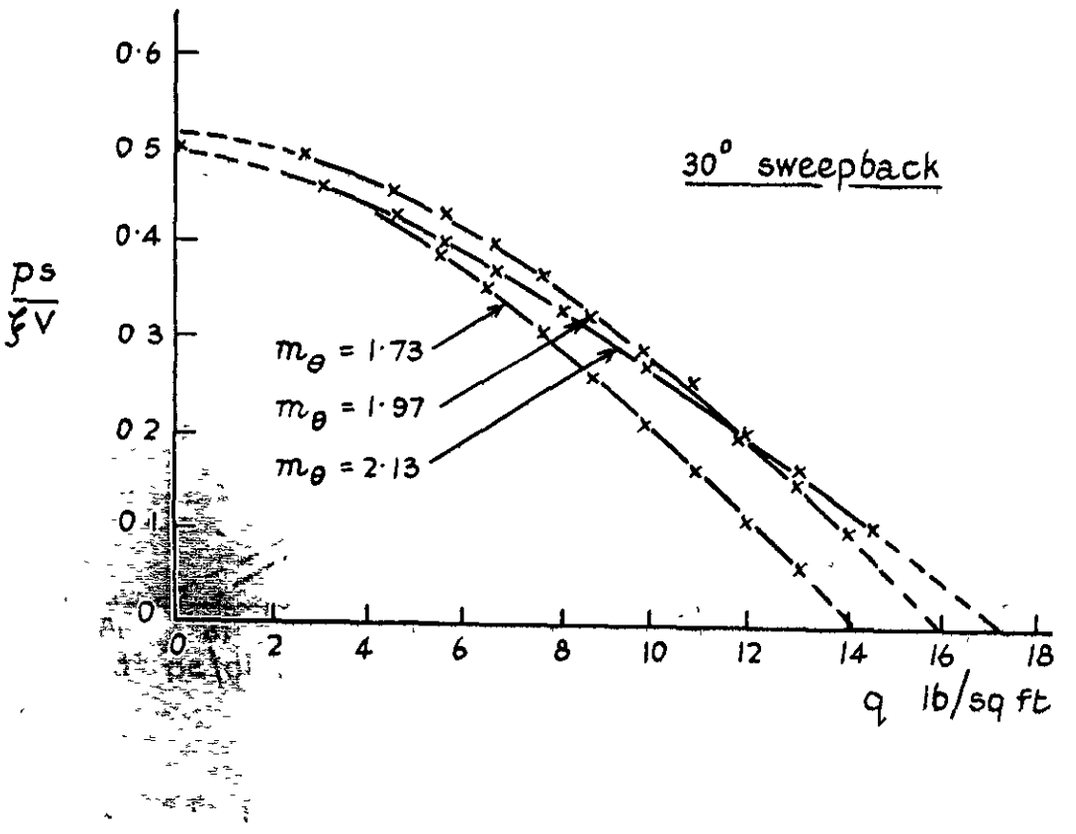


Variation of helix angle in roll with dynamic head.

FIG 7.

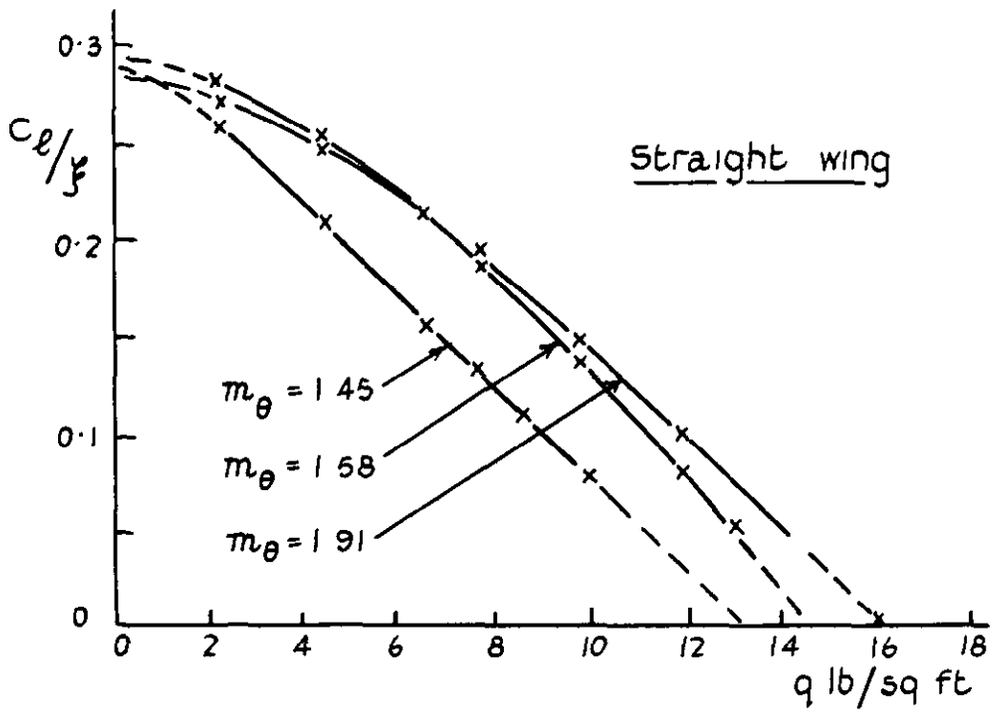


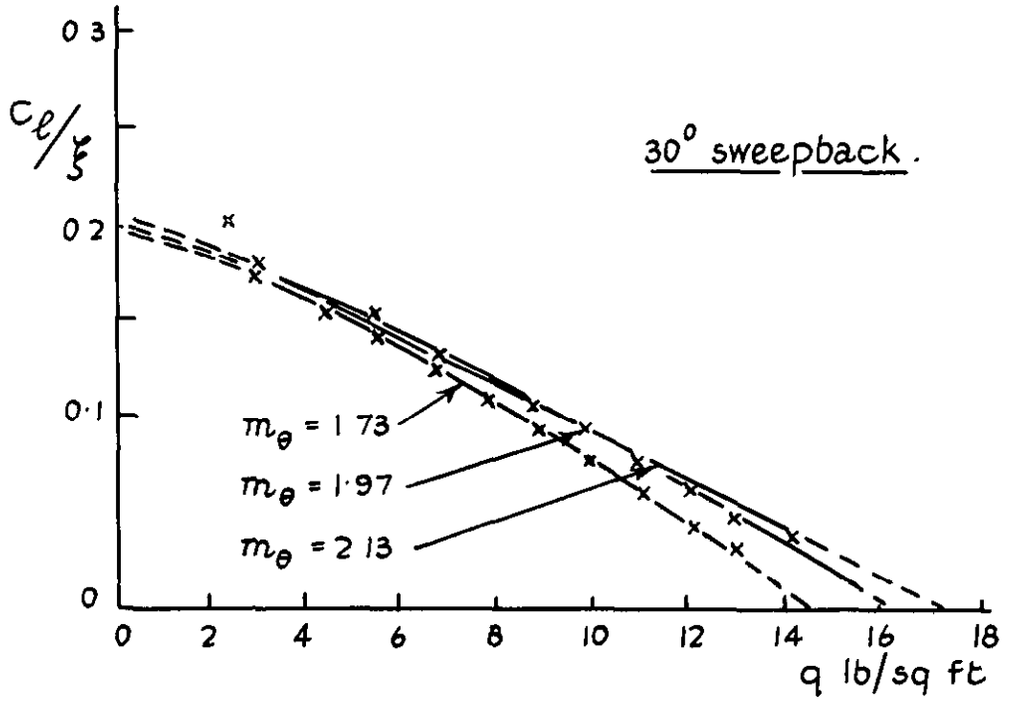


Variation of rolling moment coefficient with dynamic head.

FIG 8.

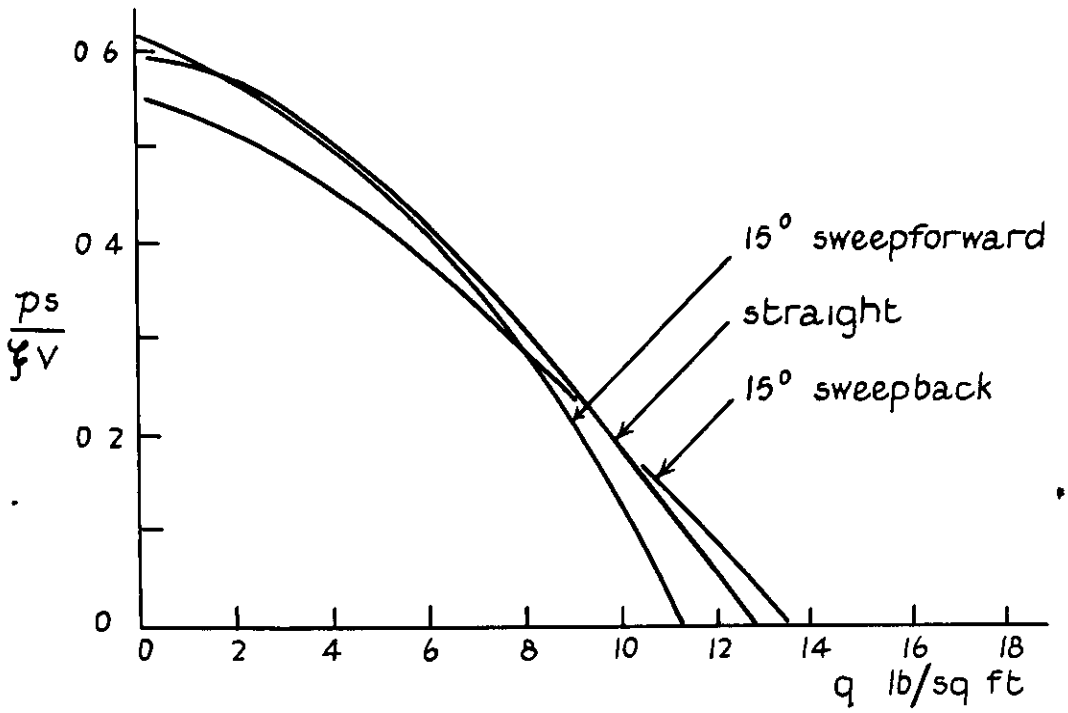


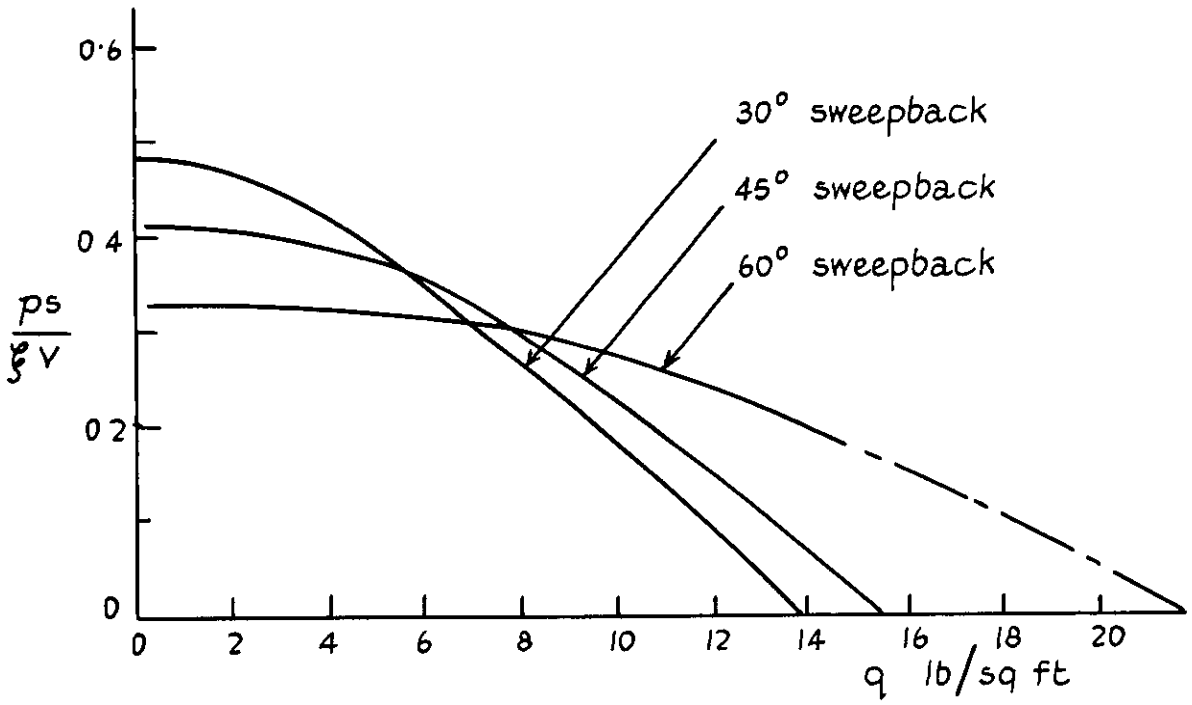


Variation of helix angle in roll with dynamic head at standard stiffness ($m_\theta = 1{\cdot}70$)

FIG. 9.

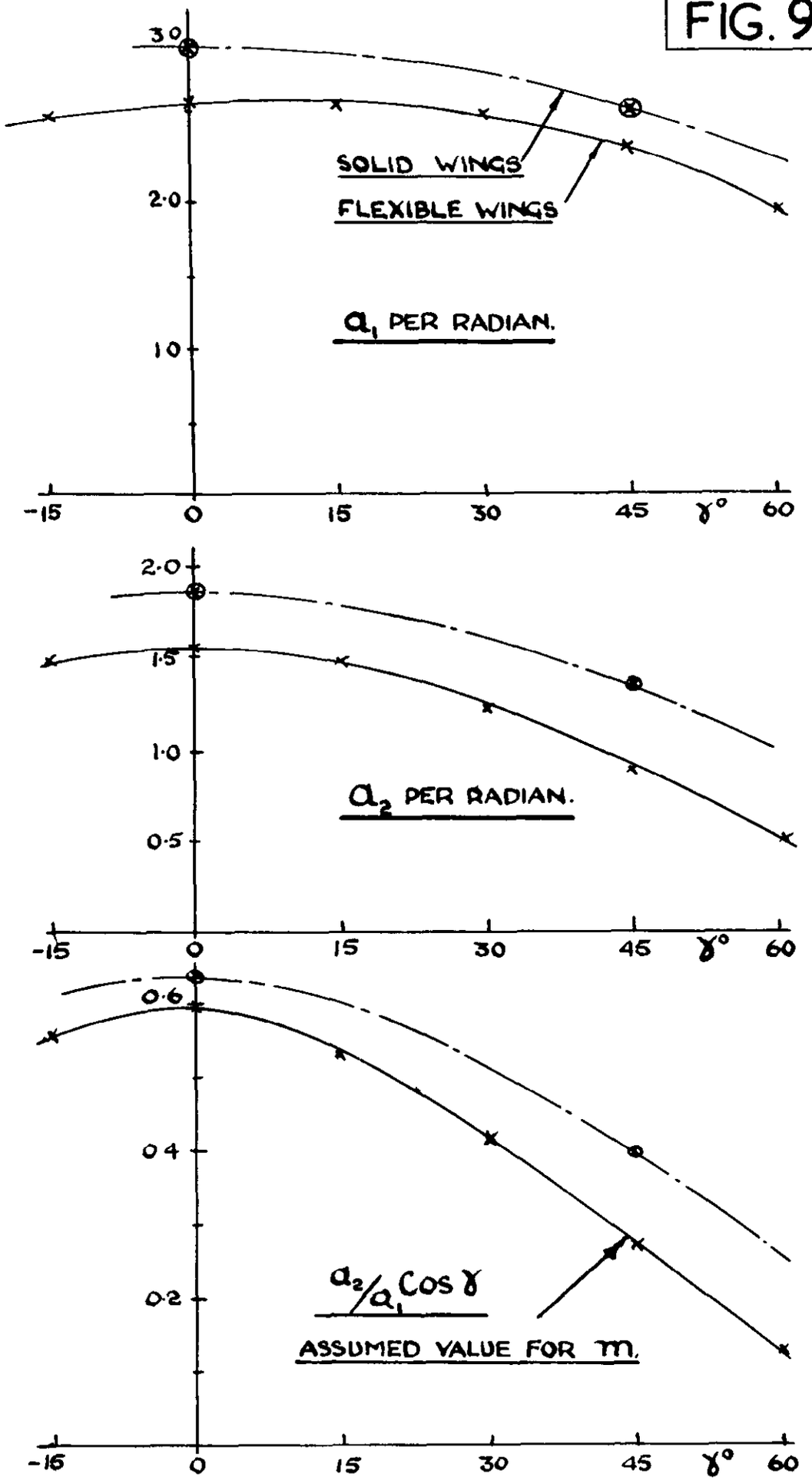


# VARIATION OF AERODYNAMIC DERIVATIVES WITH SWEEP.

16154

FIG 10.

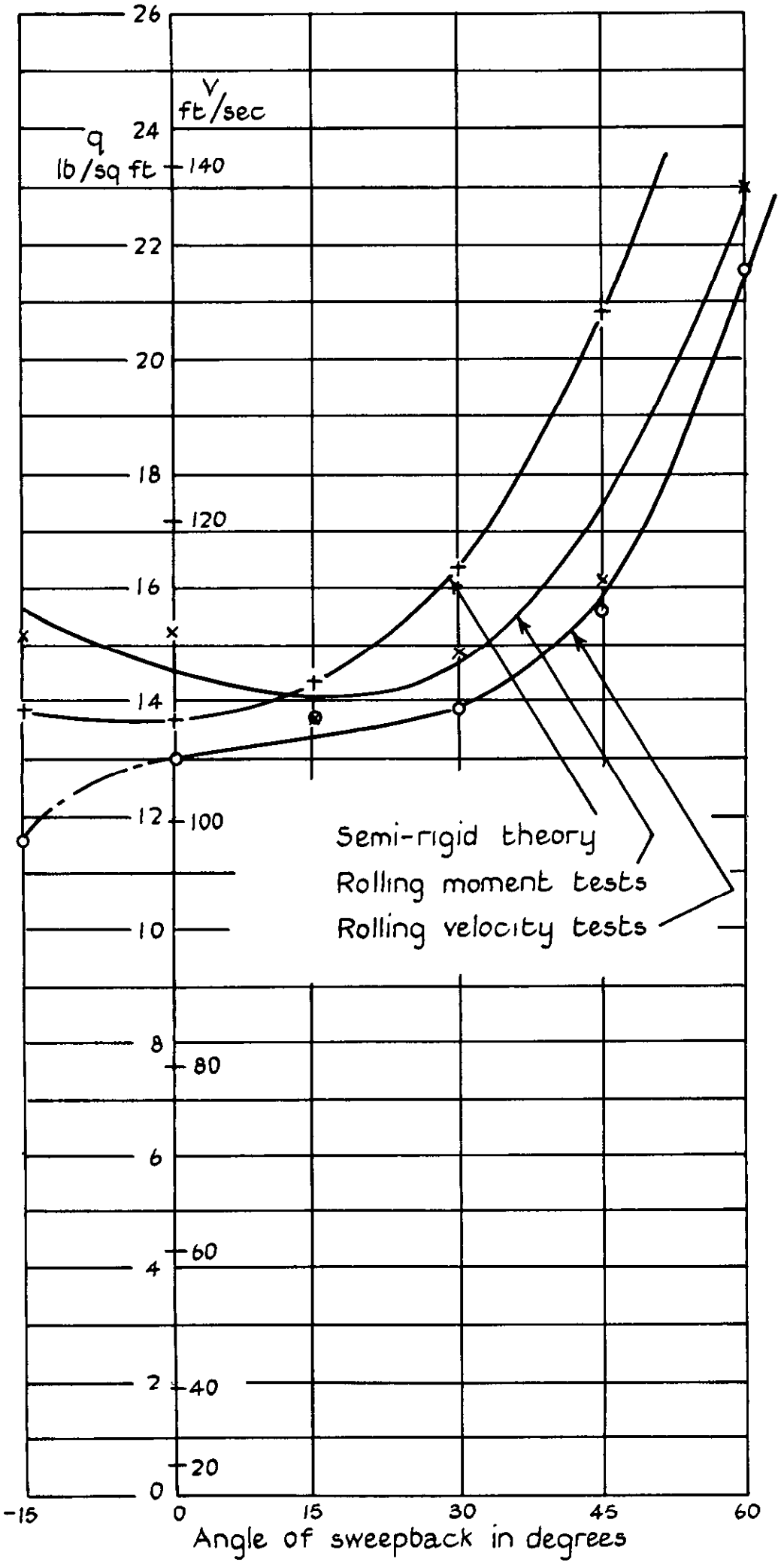


Variation of reversal speed with sweepback.

C.P. No. 159
(15,625)
A R C Technical Report



PRINTED AND PUBLISHED BY HER MAJESTY'S STATIONERY OFFICE
To be purchased from
York House, Kingsway, LONDON, W.C 2 423 Oxford Street, LONDON, W 1
P O Box 569, LONDON, S.E 1
13a Castle Street, EDINBURGH, 2 1 St Andrew's Crescent, CARDIFF
39 King Street, MANCHESTER, 2 Tower Lane, BRISTOL, 1
2 Edmund Street, BIRMINGHAM, 3 80 Chichester Street, BELFAST
or from any Bookseller
1954
Price 2s 6d net
PRINTED IN GREAT BRITAIN

S.O. Code No 23-9007-59